5-12-2014

PEG-based Fluorescent Hydrogel for Glucose Biosensing

Gayathri Srinivasan
gayathri.srinivasan@uconn.edu

PEG-based Fluorescent Hydrogel for Glucose Biosensing

Gayathri Srinivasan

B.E. Anna University, 2011

A Thesis

Submitted in Partial Fulfillment of the

Requirements for the Degree of

Master of Science

at the

University of Connecticut

2014

APPROVAL PAGE

Master of Science Thesis

PEG-based Fluorescent Hydrogel for Glucose Biosensing

Presented by

Gayathri Srinivasan, B.E.

Major Advisor _____

Dr. Yu Lei

Associate Advisor _____

Dr. Christian Brückner

Associate Advisor _____

Dr. Pinar Zorlutuna

University of Connecticut

2014

ACKNOWLEDGEMENTS

I would to like thank and express my gratitude to my Major advisor, Prof. Yu Lei for his guidance, patience and unwavering support the past two years. I have learnt a lot and grown as a student under his supervision.

Next, I sincerely thank my Associate advisors, Prof. Christian Brückner for his advice and support throughout the project and Prof. Pinar Zorlutuna for her insightful discussions on Tissue engineering and being my inspiration to work on hydrogels.

I take this opportunity to thank my previous academic mentors during my undergraduate study - Prof. K. R. Radha Krishnan, Dr. N. Sujatha and Ms. S. Sudha. I thank all my teachers for giving me the gift of knowledge.

A special thank you to the members of my lab - Dr. Liang Su, Yixin Liu, Joe Parisi, Xiangcheng Sun, Srilaya Mopidevi, Jun Chen, Xiaoyu Ma and Qiucheng Dong for their help and friendship.

Also, I would like to thank IMS associates- Dr. Pinatti, Dr. Lavigne, Dr. Zhang for helping me with the characterization techniques and Huseini of Dr. Ma's lab for help with compression analysis instrumentation.

Finally, I would like to thank my friends, here and in India for their help, love and support throughout. I wish to thank my family and cousins for their love and faith in me. Lastly, I thank Aswin Karthik for his encouragement and motivation. I would like to dedicate this to my mother, who is my best friend and my father, for being the person I aspire to be.

TABLE OF CONTENTS

List of Figures

List of Tables

ABSTRACT

Diabetes mellitus is a chronic metabolic disorder caused due to lack of insulin production by pancreatic islet cells (Type I) or underutilization of insulin produced in the pancreas (Type II). Complications arising due to this disease can be minimized by vigilant monitoring of blood glucose levels. In this study, a fluorescent enzymatic hydrogel was designed for rapid glucose detection. The glucose-responsive hydrogel was formed by polymerizing multi-arm poly (ethylene glycol), glucose oxidase and serum albumin with aminomethylcoumarin as fluorophore. The sensing mechanism relies on enzymatic catalysis of glucose, that protonates the pH sensitive aminomethylcoumarin, resulting in a fluorescence “turn-on” response. Thermal and mechanical properties of the hydrogel, with and without sensing elements were characterized. The effect of cross-linking on glass transition temperature of the hydrogels were recorded. The compression analysis of the fluorescent hydrogel shows high elasticity with good mechanical strength. Overall, a random copolymer that can be suitably modified for hydrogel based sensing is designed. At room temperature, upon addition of glucose, hydrogel sensor shows fast response time, good sensitivity and reproducibility at physiological pH. The developed fluorescence hydrogel holds great promise as an injectable glucose biosensor for in-vivo continuous glucose monitoring.

1. INTRODUCTION

Many years now, diabetes mellitus, a chronic metabolic disorder, that causes random fluctuations in plasma blood glucose concentration, has been a global pandemic. There are two main types in this disease - Type (I) caused due to lack of insulin production by pancreatic islet cells and Type (II) caused due to underutilization of insulin produced in the pancreas by the body. Statistics from International Diabetes Federation, state that, as of 2013, there are 382 million people in the world living with diabetes [1]. At this rate of disease escalation, the projected estimate of people with diabetes mellitus, for the year 2035 stands at 592 million [2]. Left untreated, diabetes has debilitating consequences including diabetic retinopathy, neuropathy, nephropathy and cardiovascular diseases which eventually lead to high rates of morbidity and mortality.

Extensive research on diabetes management shows that stringent blood glucose monitoring can delay the onset and progression of diabetes related complications and lower the diabetes associated mortality significantly [3-4]. Traditional blood glucose monitoring, which is currently in use by most diabetic patients around the world, known as self-monitoring of blood glucose (SMBG), involves glucose test trips and a handheld glucose monitor that is calibrated by patient blood samples from finger pricks [5]. A user-independent approach will alleviate most of the errors and disadvantages associated with the SMBG approach.

Continuous glucose monitoring of plasma glucose levels as opposed to self-monitoring of blood glucose involves assessing plasma blood glucose concentration

several times a day, provides information about the overall trend, magnitude of offset, causes and frequency of hypo- or hyper-glycemia [6]. The CGM approach enables the physicians and healthcare practitioners to identify plasma glucose trends for individual patients and helps to optimize treatment plans and facilitate medical action in cases of emergency.

The current designs of CGM device consists of a (i) glucose sensor that is placed subcutaneously or on the skin, (ii) a signal processing unit that processes the signal from glucose sensor and (iii) the data display unit that interfaces with the patient and provides plasma glucose trends [7-8].

1.1 Glucose sensor

Based on its contact with the body fluids and tissue, the glucose sensors utilized in the Continuous Glucose Monitoring devices can be broadly classified as reported [9-10]

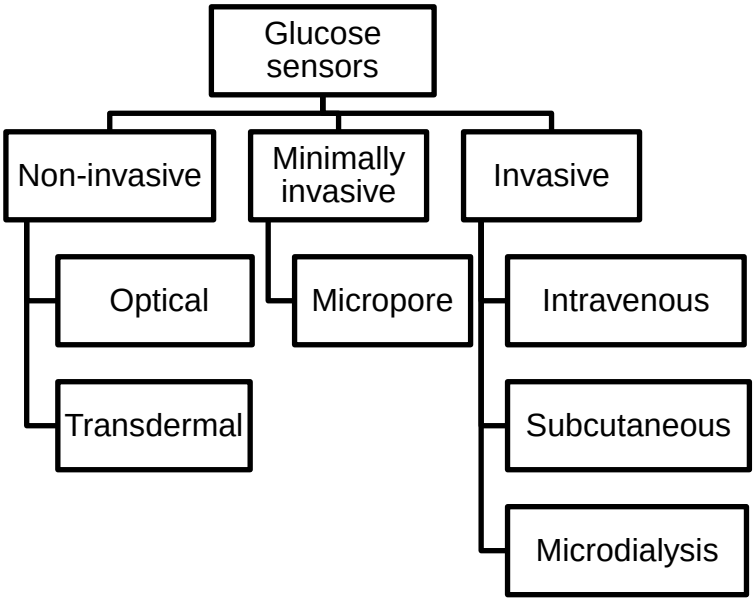

Figure 1 : Classification of Glucose sensors used in CGM devices

Of the non-invasive optical Glucose sensors, one of the most researched topics is, fluorescence based glucose sensors. Disadvantages with other detection mechanisms such as offset, calibration and low sensitivity to blood glucose concentration are overcome by fluorescence based approaches [11].

Generally, fluorescence techniques offer high sensitivity to the order of molecular resolution. When appropriate fluorophores in the near-infrared range are used, there is a great potential for non-invasive measurement. Fluorescence techniques including fluorescence decay lifetimes can be used to obtain information of the microenvironment and molecular orientation of the molecules (FRET technique) [12].

There are several molecular receptors that are inherently sensitive and specific to certain classes of saccharides and exhibit fluorescence turn-on or fluorescent turn-off reactions once the saccharide binding takes place (e.g., Boronic acid based glucose sensors) [13].

Plant lectin - Concavalin A based sensors work on the principle of competitive binding between glucose and fluorescent labeled high-molecular weight carbohydrate derivative such as dextran [14].

Glucose oxidase or other enzyme based fluorescent sensors rely on the redox reaction and the generated hydrogen peroxide or proton to change the fluorescence of the reporter molecule [15].

One of the recent advances in fluorescent based glucose sensing is Quantum dots based FRET assays. Quantum dots are semiconductor nanocrystal, predominantly of CdSe core and a ZnS shell. Desirable characteristics of Quantum dots that make

them ideally suited for glucose sensing include high quantum yield and photostability. Their broad emission spectra allow fluorescence of many different particle sizes for one excitation wavelength and hence multiplexed assays [16-17].

Despite all the advantages of fluorescence based glucose biosensors, there are few fluorescent sensors that have reached the arena of diabetes management. Major disadvantages associated with fluorescence sensors are photobleaching of the fluorophore, immune response due to the fluorophore or the fluorophore vehicle and the lag time between the actual blood glucose measurement and the sensor readout due to the interstitial fluid measurement [11, 18].

1.2 Hydrogel sensors

Hydrogels are three-dimensional, hydrophilic polymer networks that can swell and uptake large amounts of water without undergoing dissolution. This is due to stable chemical cross-links and crystalline regions in their polymer matrix. The pioneering work of Tanaka led to much interest in the field of stimuli-responsive hydrogels.

Some inherent properties are hydrogel include swelling associated volume change, high porosity, appreciable elastic modulus and phase transition in response to stimuli. Another interesting feature of hydrogels is that, depending on the application, the choice of hydrogel matrix can be modified and nature of transducing response can be tuned to suit the application. Hydrogels can be designed to undergo volumetric expansion by swelling, change color depending on the stimuli, etc.. Several sensing applications have been designed harnessing these characteristics such as across

temperature-sensitive [19] , amperometric [20], optical, pH, nature of solvent and specific ions [21].

1.3 Hydrogels in biosensing application

Inherent hydrophilic nature and very high water content of hydrogels is similar to native tissue and extracellular matrix. Generally, the high water content renders them biocompatible. However, when designing hydrogels for *in-vivo* applications, the properties of hydrogel matrix should be evaluated to avoid immune response.

Hydrophilic, mostly inert nature of hydrogel gives rise to non-specific interactions of hydrogels with enzymes and proteins has led to applications of protein entrapped hydrogel formulations for pharmaceutical applications. They are already put to a wide range of applications such as contact lenses and drug delivery vehicles [22-23].

The porous structure allows for easy diffusion of molecules and their inert interaction with protein as said earlier, make them ideal choices for a biosensor matrix that houses sensing elements [24].

1.4 Outline of thesis

The objective of this study is to design a hydrogel based fluorescent sensor array that is sensitive and specific to blood glucose with good reproducibility and fast response time. The long-term goals for this sensor includes *in-vivo* injectable hydrogel for continuous glucose monitoring.

2. DESIGN OF 3-D HYDROGEL FOR GLUCOSE SENSING

Design considerations of using star branched PEG-BSA crosslinked 3-D hydrogel for Glucose sensing

The physical properties of hydrogel make them excellent choice for biosensors. Their biocompatibility and hydrophilicity make them ideal candidates for biomedical and pharmaceutical formulations.

2.1 4-arm Succinimidyl glutarate functionalized Poly (ethylene glycol)

Succinimidyl glutarate functionalized 4-arm PEG, belongs to class of PEG-NHS esters that react with primary and secondary amines to form a stable amide bond. These NHS esters are highly reactive with a hydrolysis half-life ($T_{1/2}$) between 15-20 minutes.

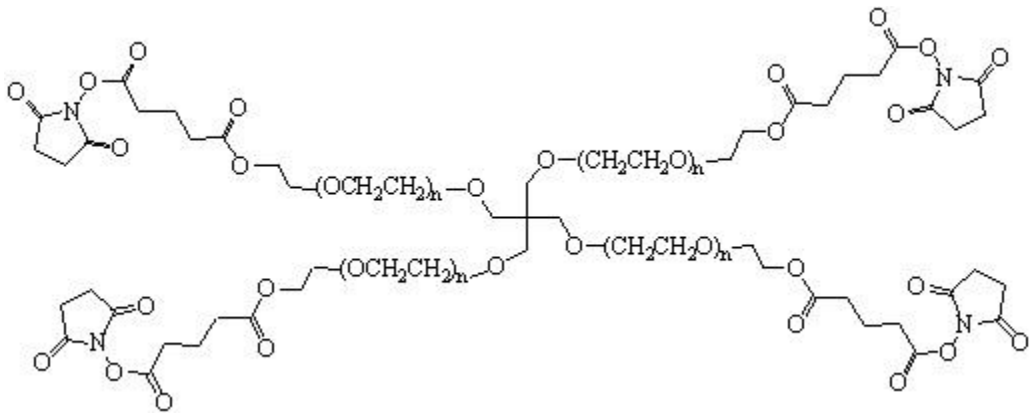

Figure 2 4-arm PEG succinimidyl gluturate ester

To Pegylate proteins, large molar excess of NHS esters are required as the reaction rate with primary amine is equivalent to hydrolysis rate, in an aqueous solution

[25]. The chemical structure of this star-branched PEG polymer has a pentaerythritol core attached to a polyethylene glycol ether and tetra succinimidyl glutarate end groups. There is a hydrolyzable O-ester bond between the glutarate and the poly (ethylene glycol) [26].

This 4-arm NHS-PEG is used in a FDA approved tissue adhesive Co-sealant®, developed by Cohesion technologies (Palo Alto, CA). The PEG-based rapid gelling system uses multifunctional star branch PEG molecules composed of tetra-succinimidyl derivatized poly (ethylene glycol) and tetra-thiol derivatized poly (ethylene glycol). Reported in 2001 [27], this compound was shown to adhere to carotid arteries, PTFE grafts *in vitro* [28]. Subsequently, in December 2001, the commercial sealant CoSeal® received FDA approval as a hemostatic adjunct during vascular reconstruction surgery.

2.2 Coumarin as fluorescence reporter

2.2.1 4-(Aminomethyl)-6,7-dimethoxycoumarin

Coumarins are derivatives of benzopyrones with a substituted keto group in the pyran ring. Heterocyclic compounds arising from the fusion of a pyrone ring with a benzene ring are a class of compounds known as benzopyrones. Two distinct types are recognized, namely benzo-α-pyrones, called coumarins, and benzo-γ-pyrones, called chromones [29]. The latter differs from the former only in the position of the carbonyl group in the heterocyclic ring.

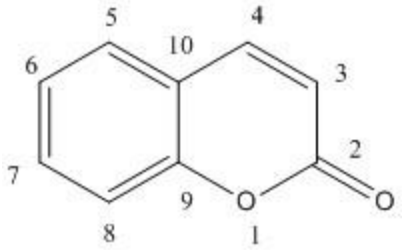

Figure 3: Coumarin numbering system

Coumarin derivatives have many advantages as fluorescent chemosensors due to their desirable characteristics including high fluorescence quantum yield (frequently above 30%) in aqueous or organic solvents, large Stokes shift, high extinction coefficients (> 18000 cm^{-1} M^{-1}), excellent light stability, and less toxicity. Generally, Coumarins are oxygen-rich compounds that are often (partially) water soluble, yet cell-membrane permeable [30].

In the study, fluorophore used, 4-(Aminomethyl)-6,7-dimethoxycoumarin was chosen for a number of physical and chemical factors. The hydrophilicity of the compound can be modified by altering the methoxy groups at positions 6 and 7 . They can be hydrolyzed and replaced with more hydrophobic groups, such as long ethers or more hydrophilic groups such as short polyethylene glycol ethers, using standard protocols [30].

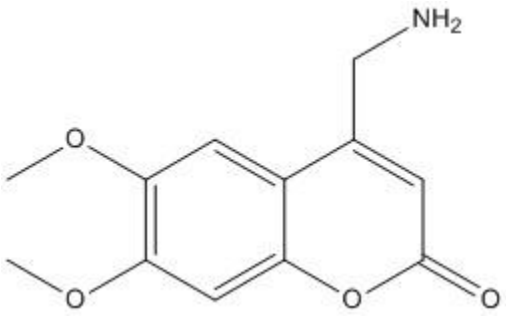

Figure 4: 4-(Aminomethyl)-6,7-dimethoxycoumarin

This fluorophore was first synthesized as a precolumn fluorescence derivatization agent for carboxylic acids in HPLC columns. The two-phase derivatization method with the benzylic amino group of the fluorophore amine was found to be of value since it suppresses background fluorescence in HPLC assays of carboxylic acids, thereby offering reasonable sensitivity and reproducibility [31]. This method is widely applied to the assay of fatty acids in human serum [32-33].

One another distinguishing property of this fluorophore (4-aminomethyl coumarins, generally) is that that they are weakly fluorescing due to a photo-electron transfer (PET) quenching process by the electron lone pair on the amine nitrogen. Upon acylation, the energy of lone pair of electrons is lowered making them unavailable for PET quenching process. Hence, the native fluorescence of coumarin is restored, exhibiting fluorescence turn-on behavior in aminomethylcoumarins.

2.2.2 The Absorption and Emission spectra of ADC 4-(Aminomethyl)-6,7-dimethoxycoumarin

Absorption Spectra

Absorption spectra of 4-(Aminomethyl)-6,7-dimethoxycoumarin (100 µM) in phosphate buffer of pH 5-8 were recorded in Varian Cary 50 UV-Vis spectrophotometer.

The fluorescence emission spectra of 4-(Aminomethyl)-6,7-dimethoxycoumarin (500 µM, DI water) was recorded in 96-well plate in Flexstation 3 microplate reader (Molecular Devices LLC, Sunnyvale, CA), with excitation wavelength at 353 nm and emission wavelength at 451 nm. The optics position was on top of the well. Spectral scan from 350-700 nm was performed for pH ranging from 3-11.

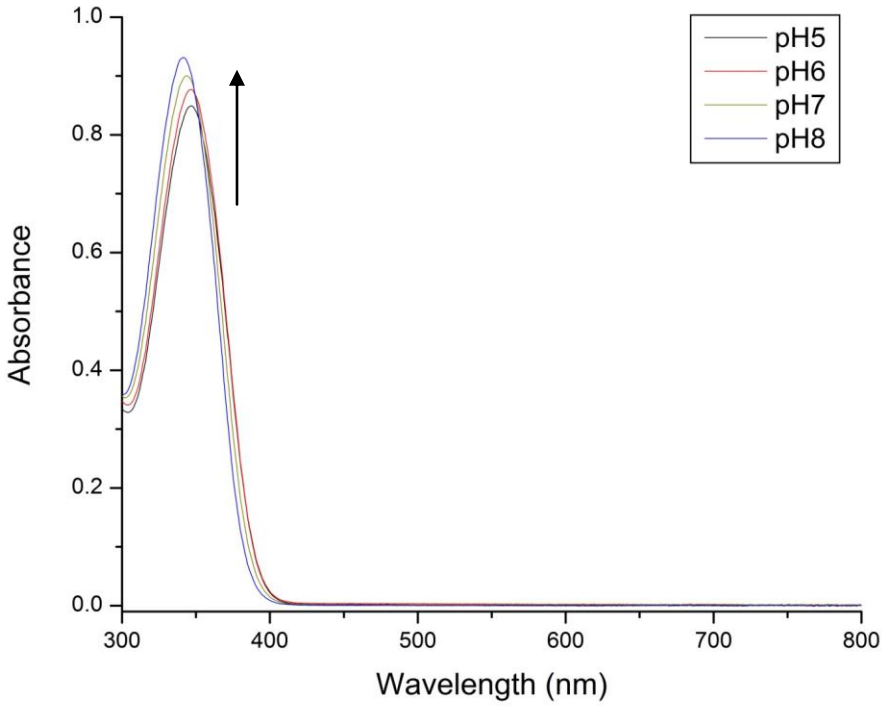

Figure 5: Absorption spectra of 4-(Aminomethyl)-6,7-dimethoxycoumarin

The pH buffers for titration from pH 3-11 were prepared as follows. 0.1 M Phosphate buffer of pH 7.0 was prepared from mono and disodium hydrogen phosphate. 1 M NaOH and HCl basic and acid solutions were used to titrate this stock solution to yield pH solutions ranging from pH 3-11, alongside a pH meter. 9:1 ratios of pH solution to fluorophore was used to test the pH sensitivity of the fluorophore. The ratio of peak intensities of the emission spectra (F) of different pH solutions with respect to least peak intensity (F_o) is used to plot Figure 6 .

From Figure 6, it is apparent that the aminomethyl coumarin shows a huge fluorescence intensity change in the pH range 7-8, which is ideal for physiological

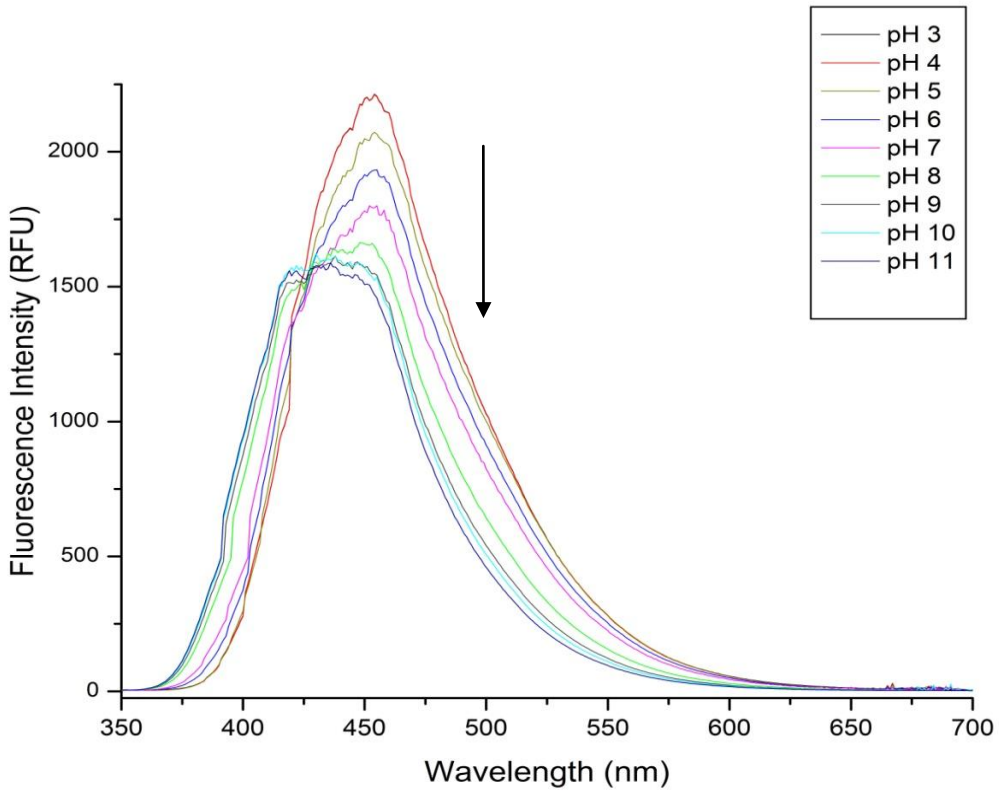

Figure 6: Fluorescence Emission spectra of 4-(Aminomethyl)-6,7-dimethoxycoumarin

chemosensing applications [34]. Also, fluorescent intensities after pH 9 are highly quenched due to intramolecular quenching of amine group in the fluorophore itself [31].

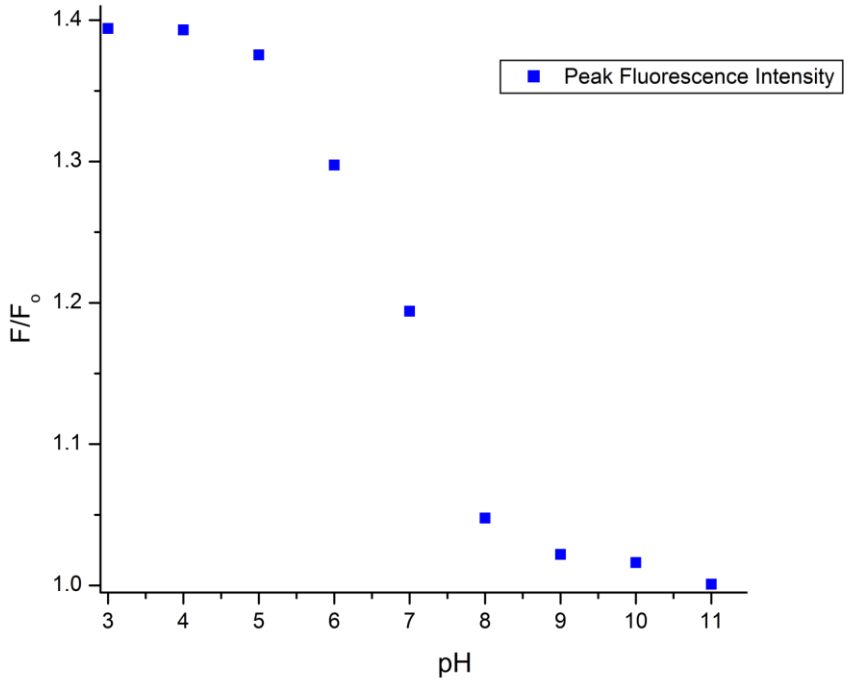

Figure 7: Normalized Peak intensities of ADC emission spectra

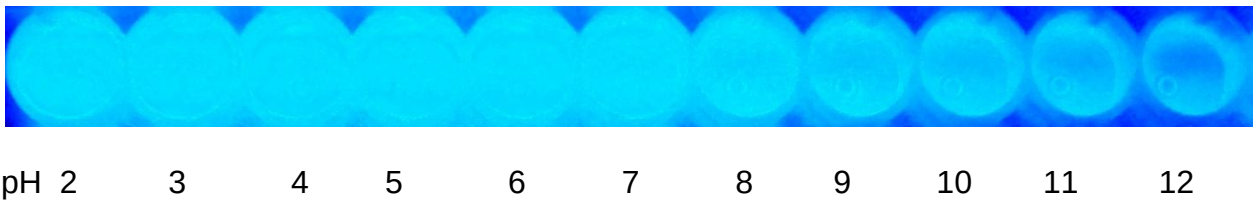

Figure 8: Microwells showing pH dependent fluorescence intensity change in 4-(Aminomethyl)-6,7-dimethoxycoumarin

2.3 Bovine Serum Albumin (BSA) for cross-linked hydrogel matrix

BSA is often used as protein concentration standard and a stabilizer for enzyme solutions in experiments. It does not affect other enzymes that do not need it for stabilization. BSA is a single polypeptide chain consisting of about 583 amino acid residues and no carbohydrates. At pH 5-7 it contains 17 intrachain disulfide bridges and 1 sulfhydryl group [35]. BSA has a molecular weight of 66,430 Da (approximately 66.5 kDa) and consists of 59 lysine residues, of which 30-35 have primary amines that can react with crosslinkers for peptide coupling.

2.4 Enzyme Immobilization

Glucose oxidase is the enzyme of choice in designing enzymatic glucose sensor. The catalysis reaction on glucose substrate reduces the FAD cofactor and gnerates gluconic acid which causes the fluorophore in this study to exhibit "turn-on" fluorescence response to increasing glucose concentration.

2.4.1 Glucose Oxidase

Glucose Oxidase is an enzyme of oxidoreductases class that catalyzes the oxidation of β-D-Glucose with dioxygen to produce D-glucono-1,5-lactone and hydrogen peroxide. Structurally, the Glucose Oxidase enzyme prepared from *A.niger* is a dimer in which two molecules of FAD (Flavin Adenine Dinucleotide - cofactor) are tightly bound per dimer. The dimer consists of 30 lysine residues with primary amines that can readily crosslink to form peptide bonds [36-37]. The following equation shows the catalysis equation of GOx.

$$E - FAD + G \rightarrow k_1 \rightarrow E - FADH_2 - P \rightarrow k_2 \rightarrow E - FADH_2 + P$$

$$E - FADH_2 + O_2 \rightarrow k_3 \rightarrow E - FAD - H_2O_2 \rightarrow k_4 \rightarrow E - FADH_2 + H_2O_2$$

3. MATERIALS AND METHODS

3.1 Materials

Four-arm Poly (ethylene glycol) Succinimidyl glutarate ester (PEG SG, MW = 10,000 Da) SG was purchased from Creative PEGworks (Winston Salem, NC, USA). Bovine Serum Albumin (BSA, Mw = 66,430 Da), Glucose Oxidase enzyme (GOx) (E.C. 1.1.3.4, 157,500 units/g, Aspergillus Niger), D-Glucose (MW = 180.16 g/mol) and PBS tablets were purchased from Sigma-Aldrich (MO, USA). One PBS pellet was dissolved in 200 mL of deionized water yields 0.01 M phosphate buffer, 0.0027 M potassium chloride and 0.137 M sodium chloride, pH 7.4 $\pm$ 0.1, at room temperature. Halogenated 4-(Aminomethyl)-6,7-dimethoxycoumarin (MW = 272.1 Da) was obtained from Brueckner's group at the University of Connecticut. It was synthesized by Delèpine reaction that yields crystalline solids with an overall yield of over 80% [38]. All chemical reagents were used without further purification.

3.2 Methods

Aqueous solution of 4-arm Poly (ethylene glycol)-succinimidyl glutarate (4-arm PEG SG) (10% w/v) was prepared by dissolving 100 mg of the solute in 1 mL 0.1 M phosphate citrate buffer of pH 4.0, immediately prior to polymerization.

Aqueous solution of Bovine serum albumin (BSA) (15% w/v) was prepared by dissolving 150 mg of solute in 1 mL of 0.1 M phosphate buffer of pH 7.0, immediately prior to polymerization.

The fluorophore 4-(Aminomethyl)-6,7-dimethoxycoumarin obtained as yellow crystalline powder (from Dr. Brueckner's group), was dissolved in distilled water.

Glucose oxidase and D-Glucose solutions were prepared by dissolving appropriate amounts of solvents in PBS buffer prepared as described earlier.

3.2.1 Preparation of 4-arm PEG SG-BSA hydrogel

To a 2 mL Eppendorf® tube, equal volumes of PEG SG and BSA solutions were added at room temperature and vortex mixed for a minute. The solution was immediately dispensed with a micropipette into the wells of 96-well plate and allowed to polymerize at room temperature.

3.2.2 Preparation of 4-arm PEG SG-BSA-Coumarin hydrogel

To a 2 mL Eppendorf® tube, equal volumes of PEG SG and BSA solutions were added at room temperature and vortex mixed for a minute. Immediately, fluorophore solution (4-(Aminomethyl)-6,7-dimethoxycoumarin, 500 μM) was added and vortex mixed for another 30 seconds. The solution was immediately dispensed with a micropipette into the wells of 96-well plate and allowed to polymerize at room temperature. To avoid photobleaching of the fluorophore, the 96-well plate was covered with aluminum foil until further use.

3.2.3 Preparation of 4-arm PEG SG-BSA-Coumarin-Glucose oxidase hydrogel

To a 2 mL Eppendorf® tube, equal volumes of PEG SG and BSA solutions were added at room temperature and vortex mixed for a minute. Immediately, fluorophore solution (4-(Aminomethyl)-6,7-dimethoxycoumarin, 500 μM) and Glucose oxidase (GOx, 62.5 μM in PBS) were added and vortex mixed for another minute. The solution was immediately dispensed with a micropipette into the wells of 96-well plate and allowed to polymerize at room temperature. To avoid photobleaching of the fluorophore, the 96-

well plate was covered with aluminum foil until further use. To retain enzyme activity, the 96-well plate was placed in 4˚C until further use.

3.3 Characterization of PEG SG-BSA hydrogel

3.3.1 Gelation time

The gelation time of hydrogels was determined using demonstrated by test tube inversion method[39]. The gelation time for (a) PEG SG-BSA (b) PEG SG-BSA-Coumarin (c) PEG SG-BSA-GOx-Coumarin were measured.

3.3.2 Surface Morphology

Surface morphology of the prepared hydrogel were studied using Scanning Electron Microscopy (SEM). PEG SG-BSA hydrogel cross-linked with Coumarin and Glucose oxidase were prepared and flash frozen in liquid nitrogen and lyophilized. Prior to imaging, the sample cross-sections were cut by razor blade and mounted on double-sided carbon tape stuck on SEM stubs. Further, the samples were Au:Pd coated for improved conductivity. Images were taken 500X magnification on JEOL 6335 Field Emission Scanning Electron Microscope (FESEM) operated at an accelerating voltage of 10 kV and 12 μA.

3.3.3 Attenuated Total Reflectance - Fourier Transform Infrared Spectroscopy

Attenuated total reflectance (ATR) infrared spectra of dry hydrogel samples and 4-arm PEG SG samples in powder form were obtained with a Thermo Nicolet IR 560 system, using a Zn-Se ATR accessory (Thermo Electron Corporation, PA). Each sample was placed against the ATR element and the spectra were collected in the

range 800–4000 cm^{-1} using 128 scans at a resolution of 4 cm^{-1}. After acquisition, the IR spectra were baseline corrected for carbon dioxide peak at approximately 2750 cm^{-1}.

3.3.4 Differential Scanning Calorimetry (DSC)

The Differential Scanning Calorimetry (DSC, TA instrument Q-20 Differential Scanning Calorimeter, New Castle, DE) technique was used to determine the glass transition temperature (Tg), fusion enthalpy of bound and free water and melting of the dried, freshly prepared and swollen hydrogel discs.

The samples were hermetically sealed in an aluminum pan. An empty pan was used as a reference. TA Universal Analysis 2000 software was used to analyze the T_g, and enthalpy of crystallization obtained from 2^{nd} heating cycle. The samples were heated at a rate of 10 °C/min from -90 °C to 40 °C. The 2nd cycle of thermograms were used to determine the glass transition temperature (T_g) of the hydrogel samples. Specifically, the Tg is determined by the reversing heat flow that describes a kinetic event, whereas the relaxation endotherm is represented by the non-reversing heat flow.

3.3.5 Thermogravimetric Analysis

Thermogravimetric analysis (TGA) is carried out using Perkin-Elmer TGA-7, to determine the decomposition rate of the hydrogels. The dried hydrogel samples were heated from 40 °C to 600 °C at a heating rate of 10 °C/min in air. The data were analyzed using TA Universal analysis 2000 software.

3.3.5 Mechanical Analysis - Compression testing

DMA controlled force - Compression

Mechanical analysis of the hydrogel samples were performed on TA instruments Q800 under Controlled force - Compression mode. A pair of compression disc clamps of 15 mm were used on uniform hydrogel discs (Diameter: 5.5 mm, Length: 2.25 mm). Constant preload force of 0.05 N and ramp force of 0.5N/min was applied upto 18 N at 25 ° C. Three sample hydrogel discs were tested for every category and mean was calculated.

3.4 *In-vitro* Glucose sensing

3.4.1 Sensitivity of hydrogel sensor to D-Glucose compared to control

PEG SG-BSA-Coumarin samples with and without Glucose oxidase were prepared and allowed to polymerize on 96-well plate to test the sensitivity of sensor to D-Glucose. To remove unreacted monomer and unbound fluorophore and enzymes on the hydrogel, the polymerized gels were washed several times and swollen on PBS buffer pH 7.4 for 3 hours. The excess PBS buffer was removed and replaced by D-Glucose and PBS buffer. PBS buffer was used as control. Gels were made in duplicate and fluorescence signal were analyzed between the pair of gels - one with Glucose (F) and one with PBS buffer (F_o). Fluorescence endpoint measurements were made in Biotek® Synergy2 Multi-mode Microplate reader with a filter pair of excitation at 340 $\pm$ 20 nm and emission at 440 $\pm$ 20 nm was used in making fluorescence measurements.

3.4.2 Response of Hydrogel sensor to different Glucose concentrations

PEG SG-BSA-Coumarin with immobilized Glucose oxidase enzyme were prepared and allowed to polymerize on 96-well plate to test the sensitivity of sensor to different D-Glucose concentrations. To remove unreacted monomer and unbound fluorophore and enzymes on the hydrogel, the polymerized gels were repeatedly washed and swollen on PBS buffer pH 7.4 for 3 hours. The excess PBS buffer was pipetted out before addition of D-Glucose solution of different concentrations and PBS buffer. PBS buffer was used as control. Gels were made in triplicate and fluorescence signal were analyzed between the pair of gels - ones with varying Glucose concentrations (F_n) and the one with PBS buffer (F_o). Fluorescence end-point spectra measurements were made in Biotek® Synergy2 Multi-mode Microplate reader with a filter pair of excitation at 340 $\pm$ 20 nm and emission at 440 $\pm$ 20 nm was used in making fluorescence measurements.

4. RESULTS AND DISCUSSIONS

4.1 Preparation of PEG SG-BSA hydrogel immobilized with Coumarin fluorophore and Glucose oxidase enzyme

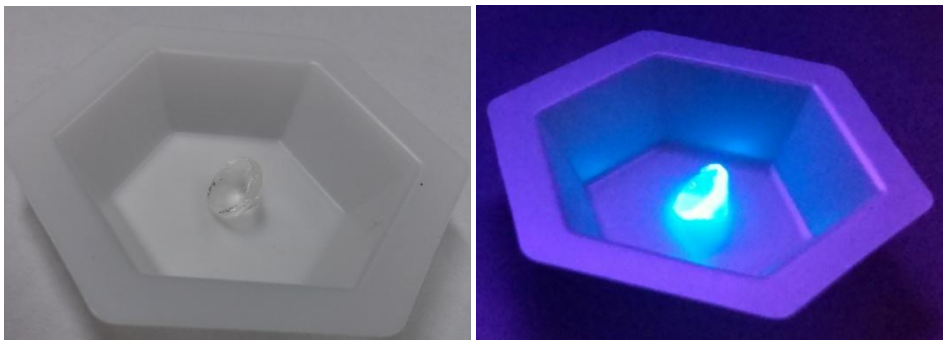

(a) (b)

Figure 9: Optically semi-transparent PEG SG-BSA hydrogel in (a) white light and (b) under UV light (wavelength = 365 nm)

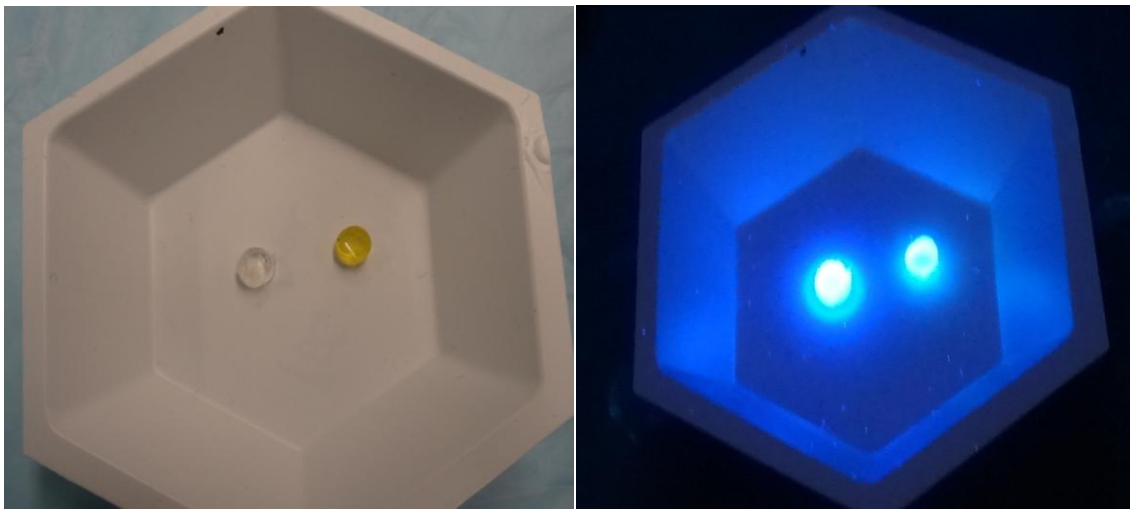

(a) (b)

Figure 10: Optically semi-transparent PEG SG-BSA Coumarin hydrogel (left) and PEG SG-BSA Coumarin GOx hydrogel (right) in (a) white light and (b) under UV light (wavelength = 365 nm), respectively.

The presence of FAD cofactor in Glucose oxidase enzyme renders PEG SG-BSA-Coumarin-GOx gels yellow which are otherwise optically semi-transparent (PEG

SG-BSA and PEGSG-BSA-Coumarin gels)[36]. The gels were firm to touch. Also, enzyme immobilization (Glucose oxidase) reduces the fluorescence of bound fluorophore to a smaller extent, as is apparent from the above Figure 10 of the gels under UV light.

4.2 Gelation time

The Gelation time determined by tube inversion method for various gels are given in Table 1. The time, when polymer solution stops flowing in inverted tubes, was recorded at 25˚C. The fast gelation time is a highly desirable characteristic for *in-vivo* injectable hydrogel sensing applications.

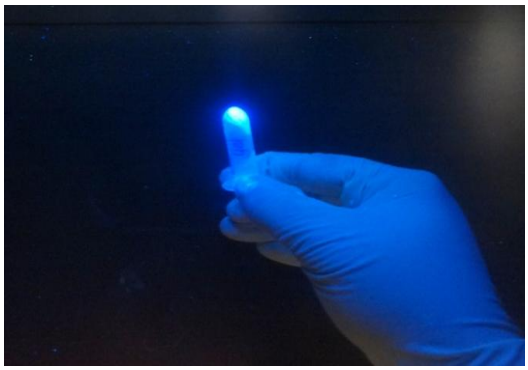

Figure 11: Representative image of gel formation on tube inversion under UV light (Wavelength = 365 nm)

Table 1: Gelation time

Gel type	Gelation time
PEG SG-BSA	12 minutes
PEG SG-BSA-Coumarin	8 minutes
PEG SG-BSA-Coumarin-GOx	6 minutes

The gelation time can be tuned by choosing appropriate solvent buffer for 4-arm PEG SG [25]. Using buffers close to pH 7, will accelerate gelation point. The gelation point is seen to increase as the total number of amino groups available for binding with 4-arm PEG SG increases (No. of amino groups in (Coumarin-BSA-GOx) > (Coumarin-BSA) > (BSA)).

4.3 Surface morphology

Surface morphology of PEG SG-BSA gel with and without enzyme and fluorophore are characterized by Scanning electron microscopy. SEM images reveal highly macroporous, homogeneous, honeycomb morphology.

The freshly prepared hydrogels were flash frozen in nitrogen and lyophilized prior to SEM imaging. These observed macropores under SEM are representative of water-filled areas. The large pore size of these gels helps in achieving faster response time - an important design consideration in hydrogel-based biosensors [40]. The SEM images also show that the pore sizes of PEG SG-BSA-GOx-Coumarin gel are slightly larger than those of PEG SG-BSA gel.

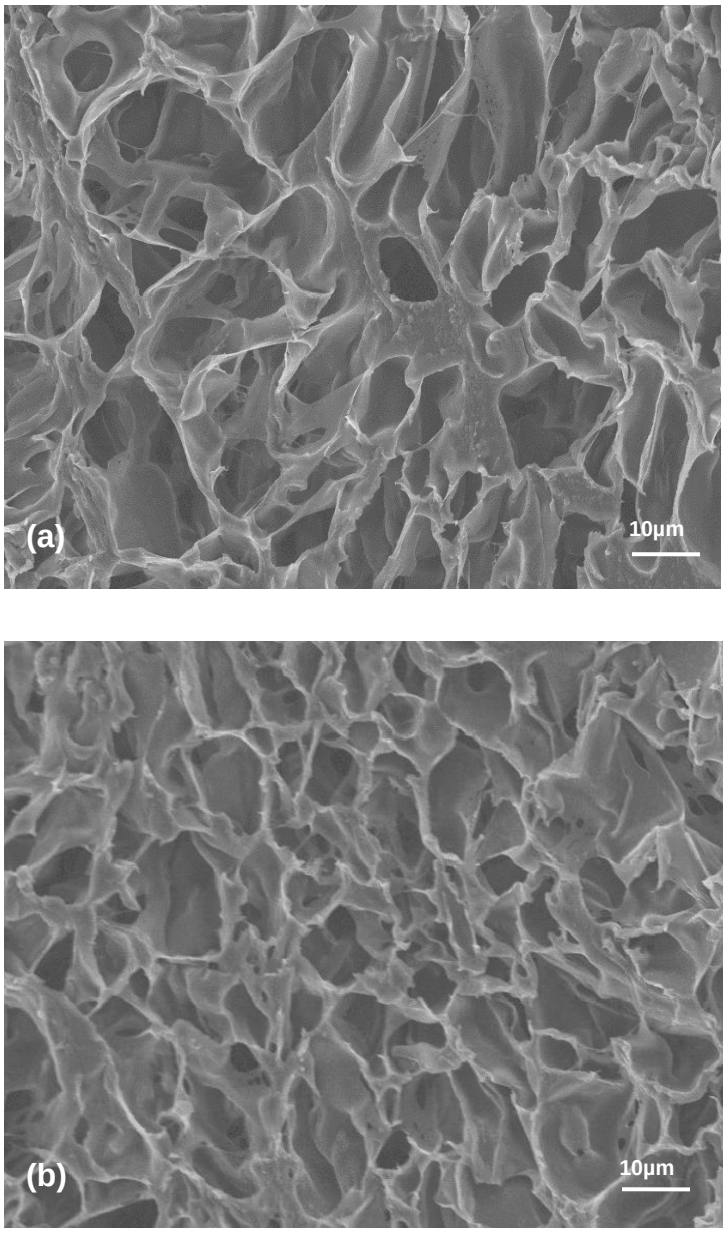

Figure 12: FESEM images of (a) PEG SG-BSA-GOx-Coumarin; (b) PEG SG-BSA hydrogels (500X magnification). Scale bars = 10 µm

4.4 Fourier Transform Infrared Spectroscopy

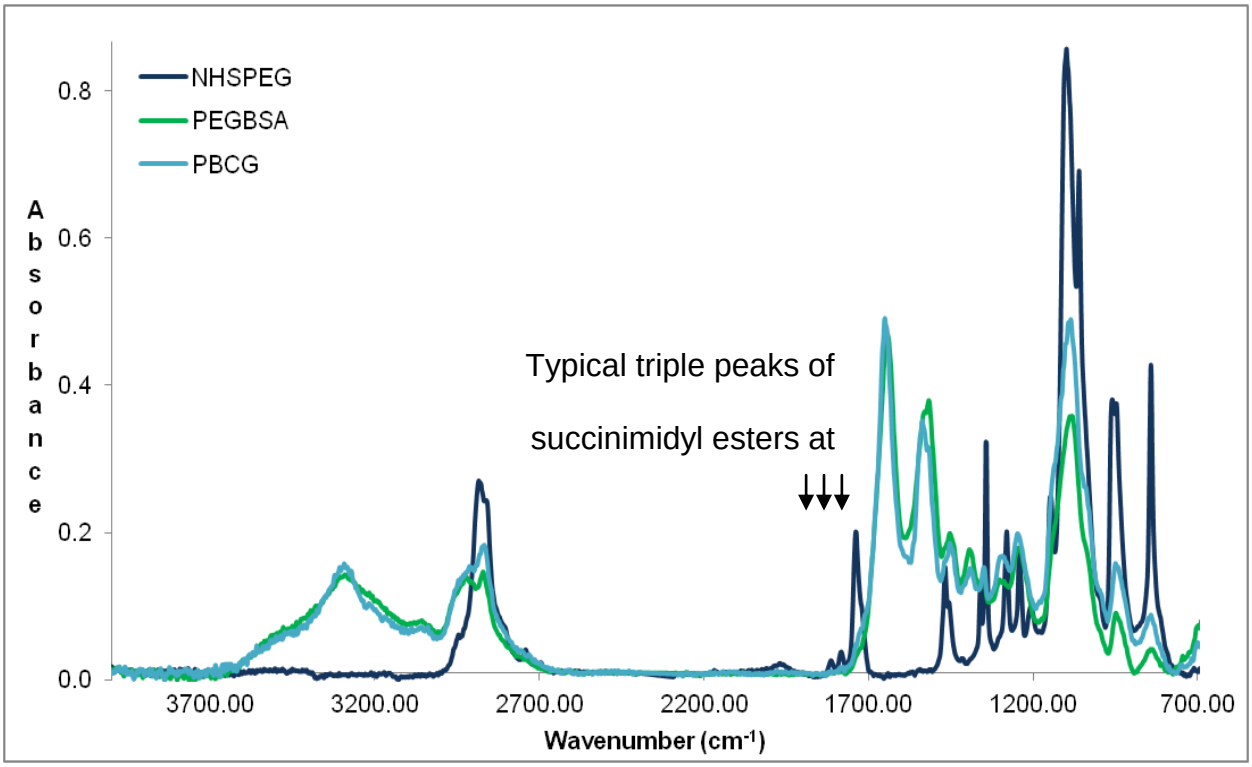

Figure 13: Overlay of IR Absorbance spectra of crystalline 4-arm NHS-PEG (——), and dry samples of PEG SG-BSA (——) and PEG SG-BSA-Coumarin-Gox gels (——). The succinimidyl ester end-groups are substituted by amide bond formation during polymerization of hydrogel and their characteristic triple peaks are missinng from the hydrogels.

ATR-FTIR technique is a popular choice in characterizing the hydrogels. The method requires little or no sample preparation and can be used for both qualitative and quantitative FTIR analysis. The thickness of sample plays no role and to evaluate water containing hydrogels ATR-FTIR is method of choice [41].

The fingerprint region of dry 4-arm PEG SG IR spectra exhibits characteristic triplet band at 1745, 1789, and 1810 cm^{-1} is caused due to symmetric and anti-

symmetric stretching of υC=O carbonyl groups of succinimidyl ester. These peaks are not observed after hydrogel formation signifying the formation of CO-NH linkage substituting NHS end-groups [42].

In the IR spectra of both the gels, a broad peak is observed at 3400-3500 cm^{-1} contributed by residual water present in the hydrogel and also N-H stretching of BSA. The peaks contributed by PEG segments are at 2932 cm^{-1} due to (C-H) stretching and 1170 cm^{-1} due to (C-O-C) stretching [43].

4.5 Characterization of Hydrogel

The complex molecular cross-linking and phase transition during hydrogel polymerization were investigated by thermal analysis techniques. An insight on the effect of each compound on the hydrogel network architecture and crosslinking is got by characterizing Differential Scanning Calorimetry (DSC) and Thermogravimetric (TGA) analysis techniques.

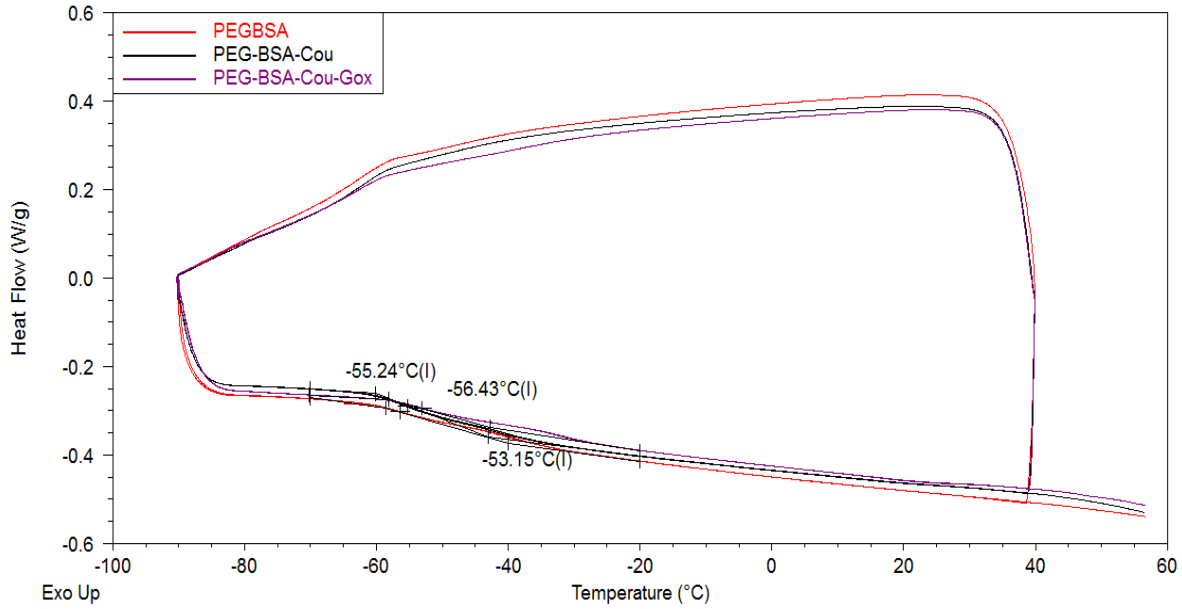

Figure 14: Overlay of DSC thermograms of PEG SG-BSA (red trace), PEG SG-BSA-Coumarin (black), PEG SG-BSA-Coumarin-GOx (purple) hydrogels showing an increase in Tg.

DSC thermograms have been widely used to study thermal transitions in polymers and polymer blends. The glass transition temperature Tg for a polymer is an indicator of the stability of the polymer above a temperature range. The PEG SG-BSA hydrogels are seen to stable at room temperatures and were tested till 40 ^{o}C. The BSA of the hydrogel matrix is denatured at temperatures 61℃ and above. Also, the immobilized heat-sensitive GOx enzyme was considered and the hydrogels were tested in the range of -90℃ to 40℃, with the objective of determining glass transition

temperature of the polymer and the different states of bound water in the hydrogel matrix.

From the DSC thermograms of dry gels, PEG SG-BSA gel structure with and without fluorophore and immobilized enzyme are very similar. A comparison of the thermograms of PEG SG-BSA gel with and without fluorophore reveals that the addition of fluorophore causes better crosslinking during polymerization. Addition of stiffer chains such as the aromatic rings of Coumarin molecule, restricts molecular translational motion, thus causing Tg to increase in PEG SG-BSA-Coumarin compared to PEG SG-BSA gel. As the composition of coumarin in the resultant polymer is low (5%), the increase in Tg is not substantial [44].

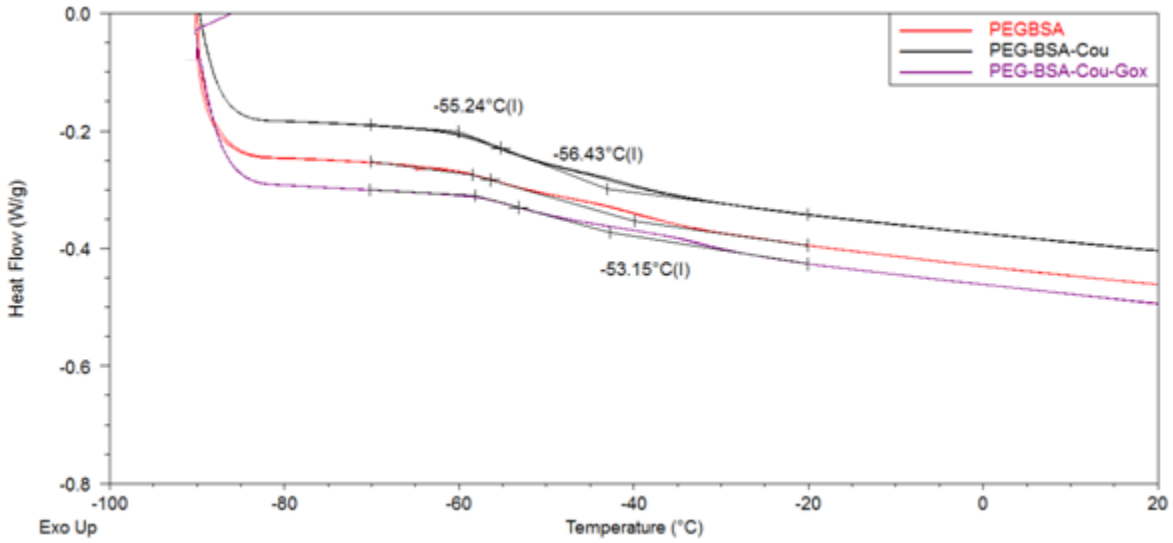

Figure 15: Overlay of glass transition regions in DSC thermograms of PEG SG-BSA (red trace), PEG SG-BSA-Coumarin (black), PEG SG-BSA-Coumarin-Gox (purple) hydrogels.

The third hydrogel with immobilized Glucose oxidase in the matrix along with coumarin fluorophore, leads to more pronounced increase in Tg. Comparing with PEG SG-BSA thermogram, its crystallinity is increased because of better cross-linking in the

polymer as the number of amino groups available for chemical coupling in Glucose oxidase makes significant contribution. This is exhibited as a smoother transitioning compared to step-wise transition in a lesser cross-linked sample.

The thermograms of all three hydrogels are very similar and are of random copolymer type [45]. The addition of fluorophore and enzyme to the polymerization mixture did not cause any phase separation. The overall crystallinity of the polymer has increased due to more restricted movements in the polymer backbone. However, the absence of a defined crystallization endotherm shows that the synthesized PEG SG-BSA gel is an amorphous polymer.

The glass transition temperatures (Tg) of all three hydrogels synthesized (i.e PEG SG-BSA, PEG SG-BSA-Coumarin, PEG SG-BSA-Coumarin-GOx gels) were determined by Differential Scanning Calorimetry (DSC) technique and are listed in Table 2.

Table 2: Glass transition temperatures of three gel types

Gel type	**Glass transition temperature (Tg) (in Celsius)**
PEG SG-BSA	-56.43
PEG SG-BSA-Coumarin	-55.24
PEG SG-BSA-Coumarin-Gox	-53.15

The swollen and freshly prepared hydrogels show distinct peaks of endotherm around 0˚C due to very high water content of PEG SG-BSA hydrogels. A fundamental characteristic feature of hydrogel is the presence of two or more states of water in them as discussed in the earlier section [46].

Interactions of hydrophilic groups lead to primary-bound water and the subsequent swelling leads to hydrophobic groups also being exposed to solvent - secondary-bound water, together termed as total bound water. The polymer network absorbs more water due to osmotic forces and covalent links and is called free water or bulk water. This is when the hydrogel is said to attain equilibrium swelling. In this study, gel was allowed to swell only for 90 minutes due to sample size restrictions. Equilibrium swelling of the gel has not been reached. However the swollen gel (black) shows a much broader peak signifying transition of water than the newly synthesized gel. It should be noted that the rate of heating affects the transition of water (Rate of heating is 10˚C/min). As the volume of bound water increases, it takes longer for the bound water to melt. Ideally, freezing exotherms and heat of fusion endotherms are sharp peaks at a defined temperature. The presence of broad peaks and tails around these peaks of the thermogram proves the presence of different states of water in the gel - the bound water transitions slower than the bulk water causing the broadening of peaks. The presence of neck/projection on the endothermic peak is believed to be due to free water phase transition in the polymerization blend.

To calculate the amount of water uptake in hydrogels, an integration of area under peak of endotherm is often used. The glass transition phase to determine Tg is more apparent in dry gels compared to newly synthesized and swollen gels as the

bound water in the network matrix acts as a plasticizer and determines the onset, midpoint (estimated Tg) and end of the glass transition phase. Moreover, the presence varying amounts of water in freshly synthesized and swollen gels can lead to incorrect estimation of Tg. Hence, dry gels were used in estimating Tg.

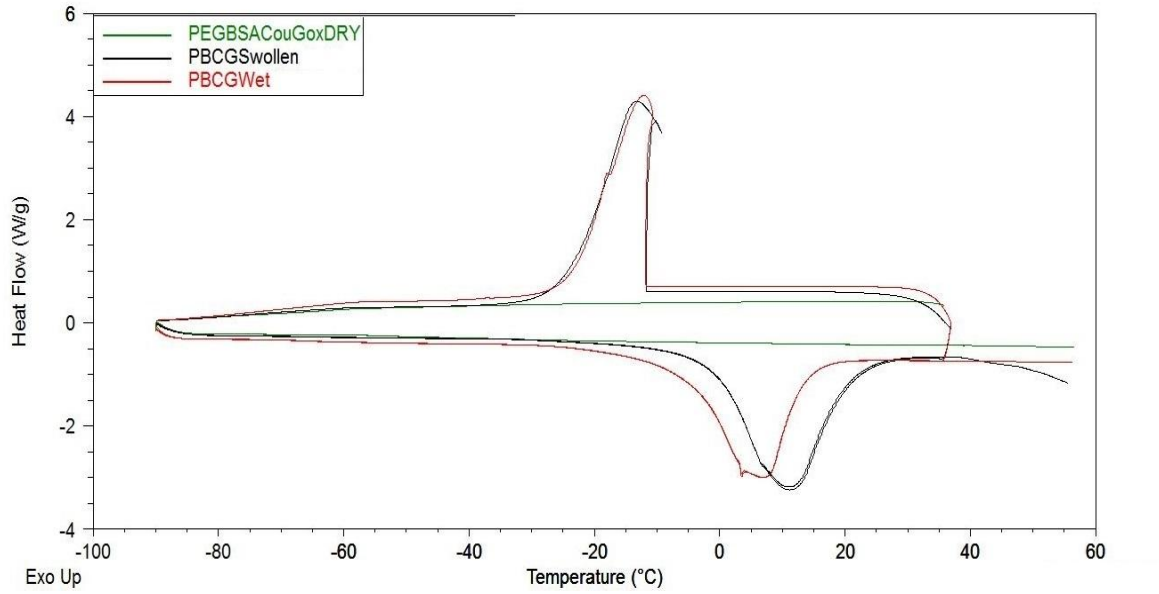

Figure 16: Overlay of DSC thermograms of PEG SG-BSA-Coumarin-GOx hydrogels in dry (green), synthesized (red) and swollen state (black) showing an increase in area under endothermic peak.

The swelling related volume increase in the three categories of hydrogels shows the differences in swelling ratios and amount of water intake for the same time and similar sample sizes. All three categories of hydrogels were swollen for 90 minutes and the sample sizes were 10 mg each before they were allowed to swell in water. It is evident from the thermograms that PEG SG-BSA-Cou-GOx gel swells the least. Tighter cross-linking causes lesser mobility of side chains and more crystalline structure compared to the other two hydrogel samples, leading to lesser access for the water

molecules to hydrophilic and hydrophobic groups that leading to lower swelling in the PEG SG-BSA-Cou-GOx gels [47].

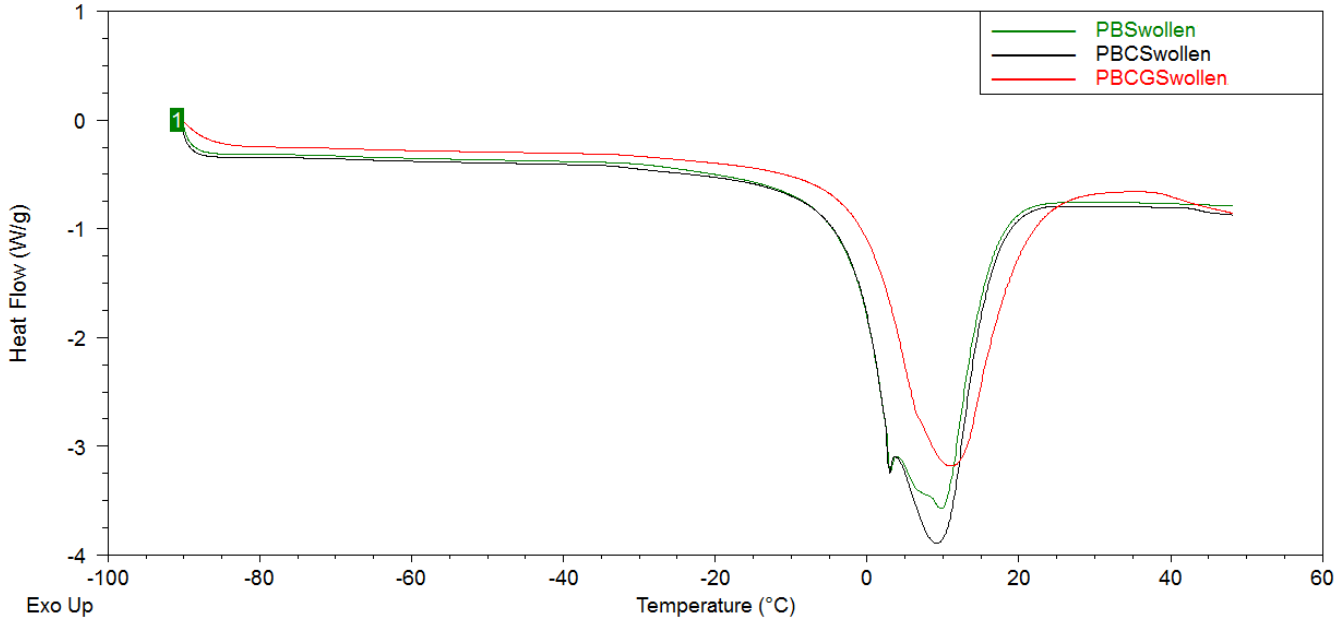

Figure 17: Overlay of DSC thermograms of swollen hydrogels - PEG SG-BSA (green), PEG SG-BSA-Cou (black) and PEG SG-BSA-Cou-GOx gel (red)

TGA measures continuous weight changes of polymer in a controlled atmosphere (e.g., air or nitrogen) as function of increasing temperature at a programmed linear rate. Thermo gravimetric analysis of two hydrogel samples (PEG SG-BSA and PEG SG-BSA-Cou-GOx) was performed under nitrogen atmosphere from 20 ^{o}C to 600 ^{o}C, at a heating rate of 10 ^{o}C/min.

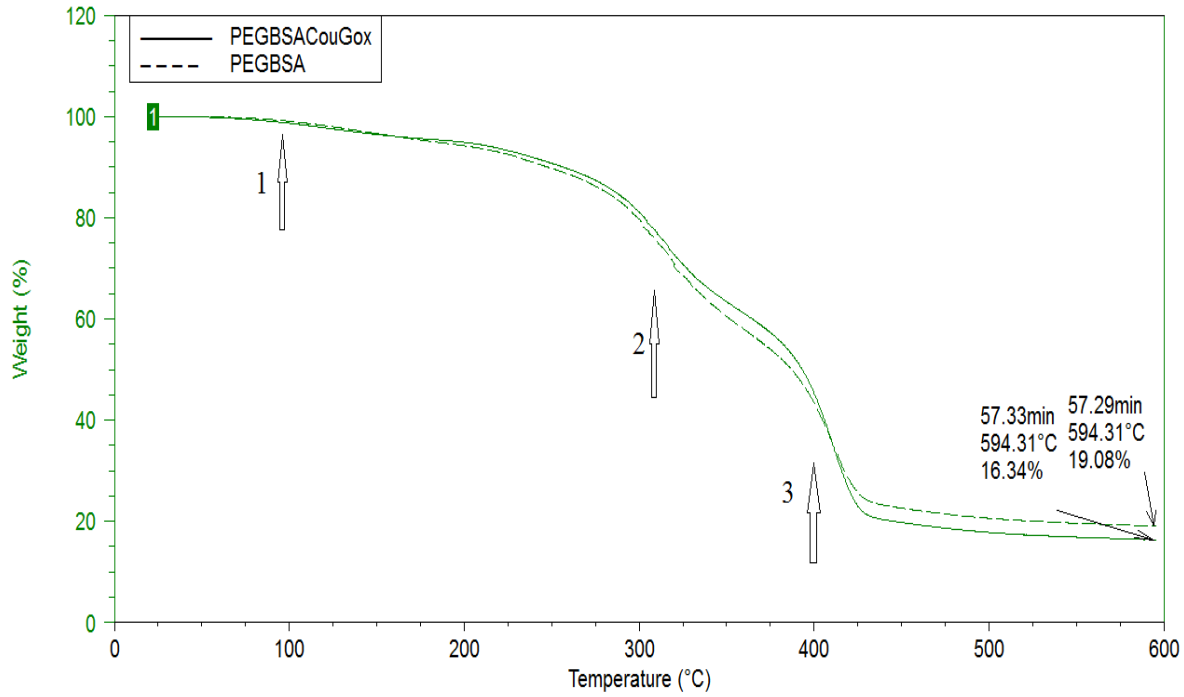

Figure 18: Overlay of TGA traces of PEG SG-BSA (dashed lines) and PEG SG-BSA-Cou-GOx (bold line) gel. Arrows mark the three distinct weight loss-regions.

From Figure 18, there are three distinct weight-loss events for both types of hydrogel. The first region is around 100 ^{o}C caused due to evaporation of residual bound water in the hydrogel matrix. The second distinct weight-loss for both the hydrogels is around 300 ^{o}C can be assigned to the degradation of amine content in the enzyme (glucose oxidase) and protein (BSA) matrix of the hydrogel [48]. Consequently, the PEG SG-BSA trace shows a lower weight derivative compared to the hydrogel with fluorophore and immobilized enzyme. The third distinct region of weight loss of the hydrogel sample corresponds to temperatures just above 400 ^{o}C, due to thermal degradation of aromatic rings in coumarin [49]. As expected, the char yield of PEG SG-BSA is slightly higher owing to the higher ratio of carbon compared to PEG SG-BSA-

Coumarin-GOx gel which has higher nitrogen and oxygen content (due to the immobilized enzyme).

The TGA traces along with the derivative of weight percentage as a function of temperature is shown in Figure 19. The addition of fluorophore and incorporation of the enzyme in the polymer blend of the hydrogel matrix (PEG SG-BSA) did not create any separate distinct phase or change in the sample morphology as proven by the TGA traces. Increasing cross-linking density improves the thermal stability as shown by the lower char yield in PEG SG-BSA-Cou-GOx gel [48].

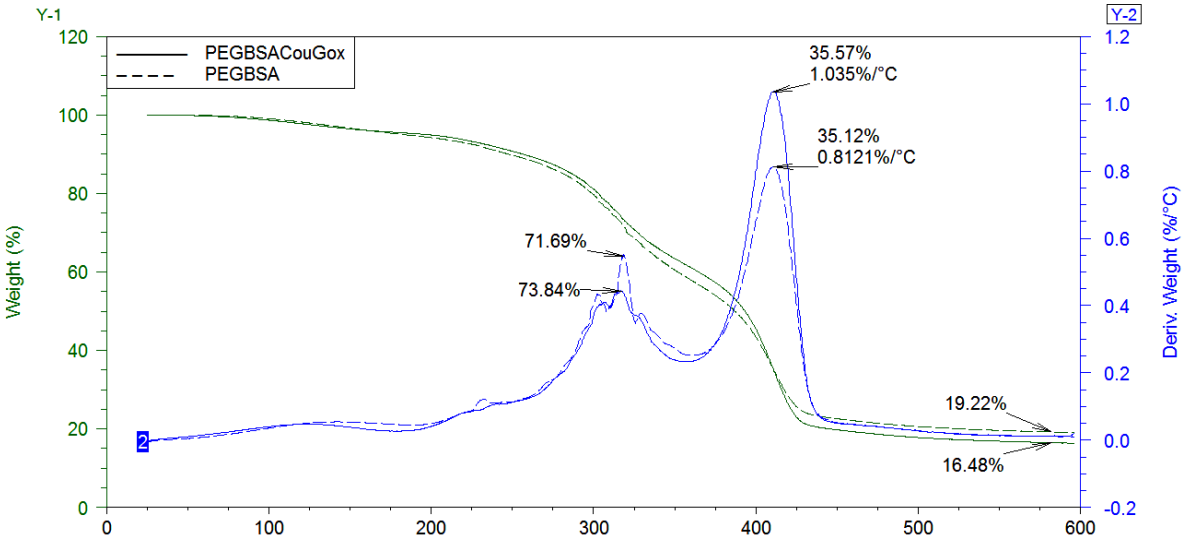

Figure 19: : Overlay of TGA traces of PEG SG-BSA (dashed lines) and PEG SG-BSA-Cou-Gox (bold line) gel

Mechanical testing - compression analysis was carried out in TA Instruments DMA analyzer. To ensure uniform sample sizes, hydrogels cast on the 96-well plate of

same sample volumes were used. After polymerization, the gels were measured for the diameter uniformity. At least three samples per category of hydrogel were tested.

The mechanical integrity of a sensor, especially pliable for materials such as hydrogels, is an important design specification *in-vitro* and *in-vivo* application. In *in-vivo* application, the hydrogel sensor should be biocompatible and pliable enough to coexist with surrounding tissue and possess enough structural integrity to withstand intraluminal and subcutaneous pressure from surrounding structures. Using monomers of higher molecular weight leading to better cross-linking efficiency is known to increase the mechanical properties of hydrogels [50].

For various hydrogel applications used in-vivo, such as drug delivery and tissue engineering applications, compressive modulus has been shown to be as low as 1 KPa for a variety of drug delivery devices [51-56]. In this study, preliminary compressive testing on PEG SG-BSA hydrogels were done and compressive stress of up to 18 N was applied.

The dependence of mechanical properties of hydrogels on network chemistry and molecular cross-linking is well documented in literature [57]. The PEG SG-BSA hydrogels synthesized in this study have strong peptide bonds between the amino groups of proteins and NHS ester of PEG SG.

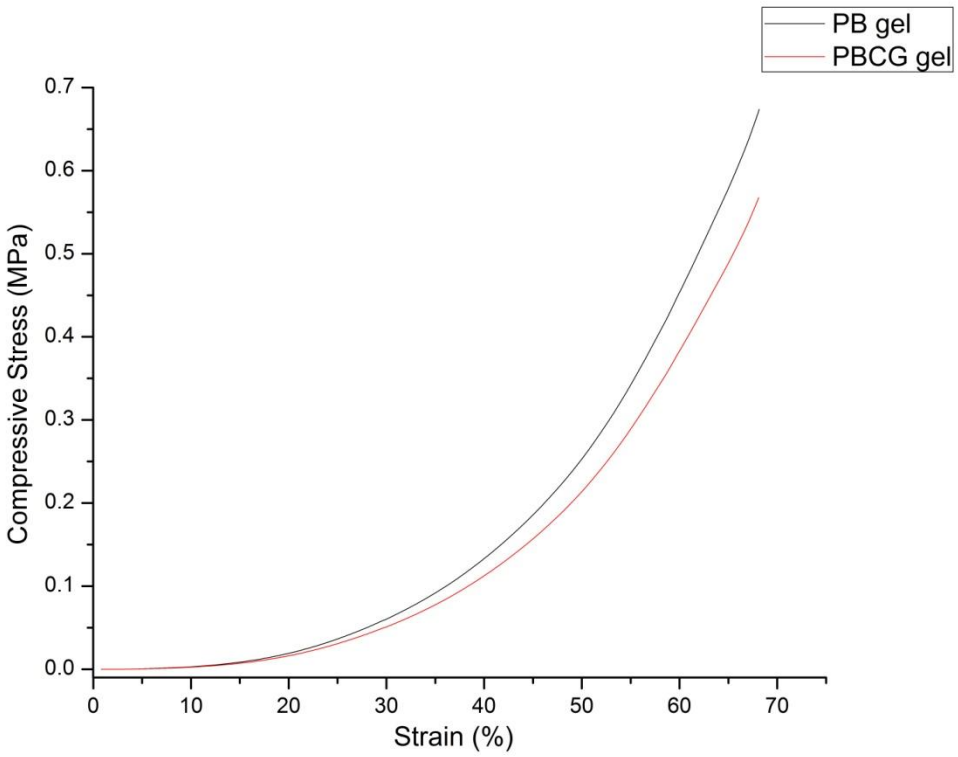

Figure 20 Overlay of compression analysis stress-strain curves - PEG SG-BSA (black) and PEG SG-BSA-Cou-Gox (red).

The stress-strain characteristic of PEG SG-BSA hydrogel with and without fluorophore and immobilized enzyme were very similar with the latter showing slightly better resistance as depicted in Figure 20, These stress-strain curves lack a linear region, hence Young's modulus of compression cannot be computed. The Young's modulus characterizes the pure elastic domain of a material where the deformation due to applied stress is reversible [46]. These mechanical stress-strain tests were investigated under a constant compression rate by measuring compressive stress and deformation until a breaking point of the gel could be achieved. However, up to 18 N, the breaking point of the gels could not be observed. The high molecular weight of the

polymer sample with extensive covalent bonds and water retention has lead to a hydrogel with very high mechanical and tensile strength.

Further tests with faster compression ramps and more number of samples should be carried out to determine the breaking point of these gels. Also, dynamic mechanical analysis with varying stresses of different frequencies will help determine the loss and storage modulus of the hydrogel. The glass transition temperature of the hydrogel can also be computed by this method as an adjunct to DSC [58].

4.6 *In-vitro* Glucose sensing

The synthesized PEG SG-BSA hydrogel with immobilized glucose oxidase enzyme and coumarin fluorescent reporter dye was tested for its sensitivity and specificity to glucose. Although, using an enzyme immediately renders the sensor specific to the analyte to be detected, chemically crosslinking the enzyme in the hydrogel matrix could have altered the active site or reduced the enzyme activity.

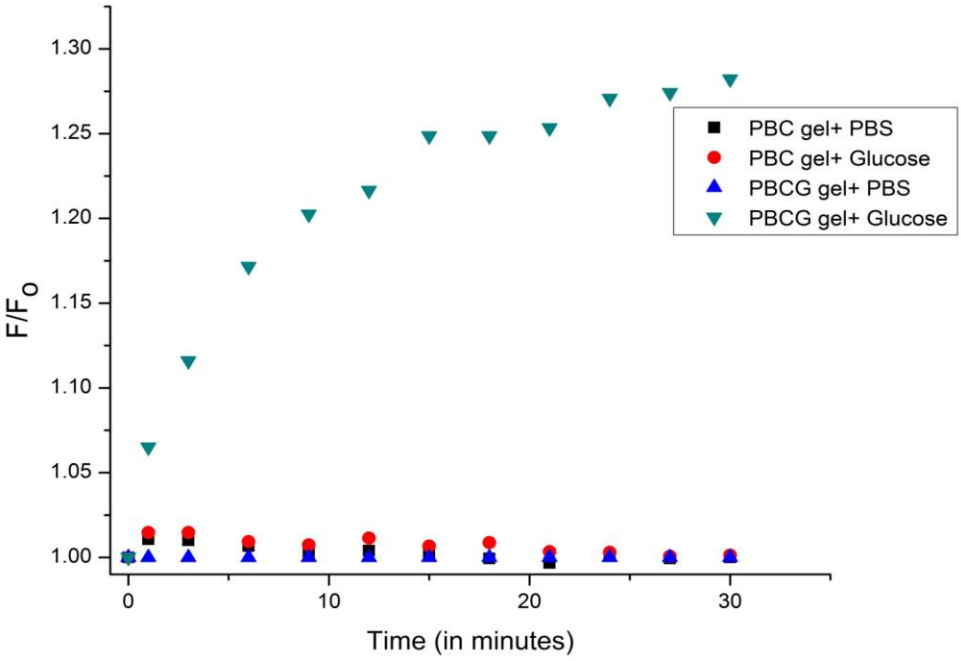

Figure 21: Hydrogel samples with and without immobilized enzyme were tested with Glucose and control (PBS buffer). The measurements were conducted at 25˚C.

Another possibility that needs to be evaluated in analyte sensing, to avoid spurious results, is that there should be no interference to the sensing from other chemicals in the sensing environment.

To ensure that the hydrogel sensor designed meets these conditions, three samples each of hydrogel with and without immobilized glucose oxidase were prepared

on a 96-well plate. Each sample of hydrogel was prepared by pipetting 80 μL of polymerization solution into the hydrogel well. To ensure the sensing data is due to enzyme activity and achieve faster response time, the hydrogels were incubated with 240 μL of PBS buffer in each well for 2 hours after synthesis. This caused the gels to swell and uptake water. Before testing, the water on top of the gels, was pipetted out and the baseline fluorescence value was tested. Subsequently, 30 mM glucose solution (solvent: PBS buffer) and control (PBS buffer) solutions were added to the swollen hydrogels. Fluorescence endpoint spectra for the hydrogels were obtained continuously on Biotek® microplate reader to observe the immobilized enzyme activity in the hydrogel sensor.

As depicted in Figure 22, the hydrogel sensor with immobilized GOx shows immediate response to Glucose as early as three minutes after the solvent added compared to others. Over time, the sensor exhibits first order enzyme kinetics and the enzyme activity achieves saturation in 15 minutes after the analyte (Glucose and Control solution) was added. The other hydrogels without immobilized enzyme showed no response. The other hydrogel with immobilized enzyme to which PBS buffer was added also showed no response. This is indicative of the activity of immobilized enzyme in the hydrogel. Thus, the enzyme in the hydrogel is active and is sensitive and specific to glucose and no other compound used in the sensing environment is seen to interfere with the synthesized hydrogel.

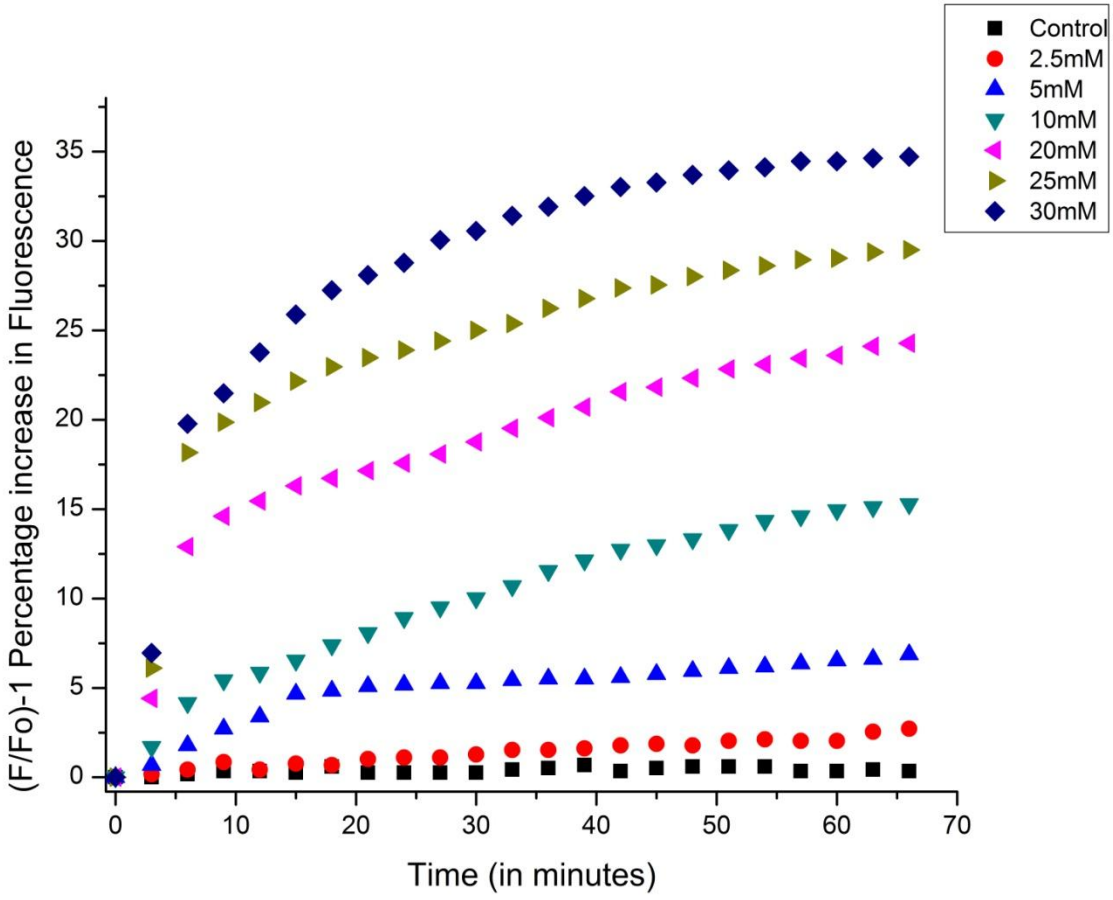

Figure 22: Time dependent Percentage increase in fluorescence response of the glucose sensing hydrogel. The concentrations of the glucose were 0 mM (■), 2.5 mM (●), 5 mM (▲), 10 mM(▼), 20 mM (◀), 25 mM (▶), 30 mM (◆). The control used was PBS buffer (pH 7.4). The measurements were made at 25˚C.

In order to test the feasibility of the sensor for real-time glucose monitoring, the hydrogels as described in earlier section, were allowed to polymerize onto 96 well-plate. Each sample of hydrogel was prepared by pipetting 80 μL of polymerization solution into the hydrogel well. To ensure the sensing data is mainly due to the enzyme activity and achieve faster response times, the hydrogels were incubated with 240 μL of PBS buffer for 2 hours after synthesis. This caused the gels to swell and uptake water.

Before testing, the water on top of the gels, was pipetted out and the baseline fluorescence value was tested.

Six glucose concentration solutions in the physiological range were tested along with control (PBS buffer) on the PEG SG-BSA-Coumarin-GOx hydrogel. Immediately after injection, fluorescent endpoint spectra readings were measured continuously using Biotek® microplate reader. Endpoint fluorescent measurements were taken continuously to observe the time dependent fluorescent response of the hydrogel to various glucose concentrations. The control hydrogel had PBS buffer solution.

As depicted in the Figure 23, the hydrogel sensor has a rapid response time. The fluorescence response shows in as low as 3 minutes after injection. The lower concentration of glucose solution gets resolved faster than the higher concentration. However, a clear trend amongst glucose concentrations is resolved in 15 minutes and is stabilized.

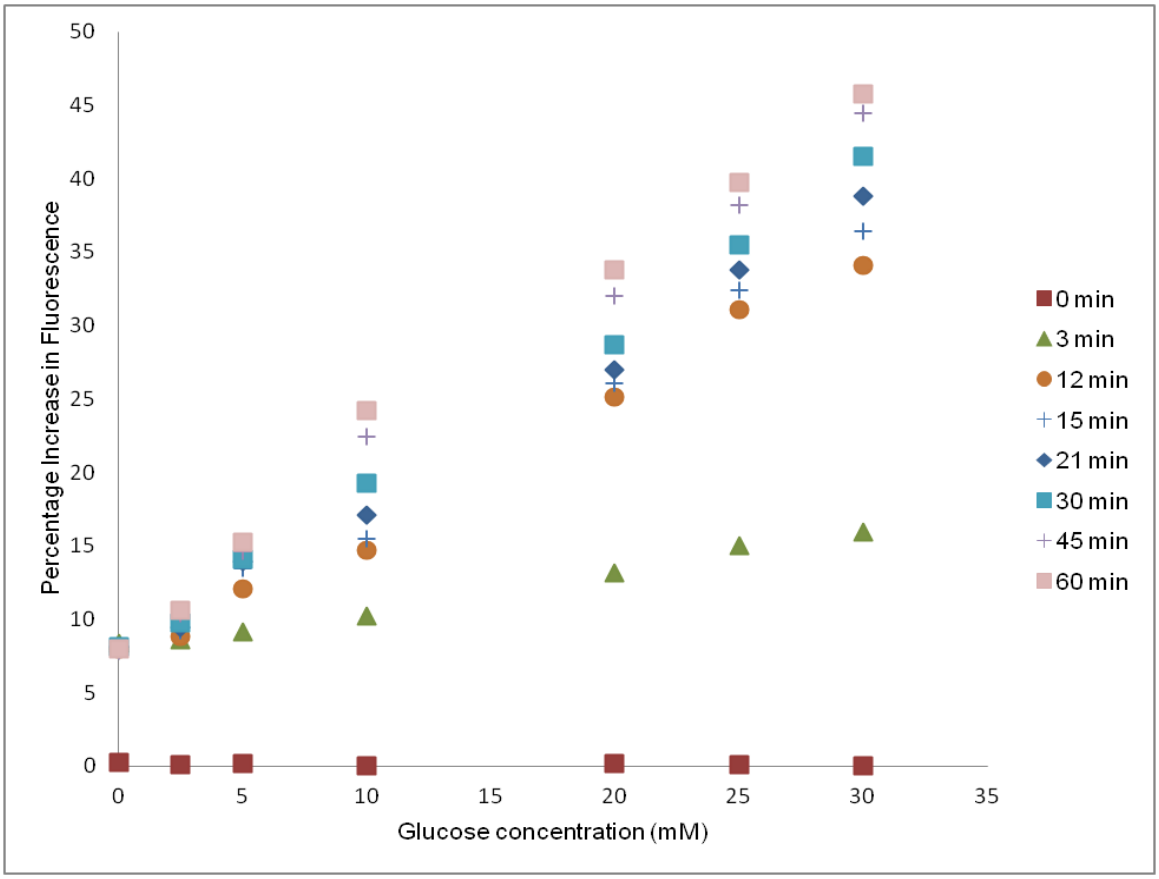

Figure 23: Percentage increase in fluorescence response of the glucose sensing hydrogel as a function of glucose concentration at different time instants. With increasing time, fluorescence intensity among the different concentrations of glucose is better resolved.

The percentage increase in fluorescence response of glucose sensing hydrogel as a function of glucose concentration at various time intervals is plotted in Figure 23. The lower glucose concentrations achieve maximum fluorescence in less time and stabilize. Higher concentrations of glucose, such as above 20 mM, take longer time to reach fluorescence maximum intensity. However, compared to other fluorescent glucose biosensors, the designed hydrogel sensor shows rapid response time and good resolution in the physiological glucose concentration range.

5. CONCLUSIONS

A 3-D hydrogel was synthesized from 4-arm PEG SG and BSA as matrix, cross-linked with 4-aminomethyl-6,7-dimethoxycoumarin and immobilized with Glucose oxidase enzyme. The succinimidyl end groups form stable peptide bond with amine residues in the BSA, fluorophore and Glucose oxidase enzyme. The polymerization at room temperature of the hydrogel was rapid. The NHS end-group substitution leading to amide bond formation was characterized by FTIR spectroscopy. The synthesized hydrogel with and without fluorophore and enzyme crosslinking was characterized by thermal Analysis techniques - Differential Scanning Calorimetry and Thermogravimetric analysis. Glass transition temperature, Tg and nature of polymer synthesized were evaluated. Preliminary results of mechanical compression analysis of the hydrogels exhibits high mechanical integrity. Finally, the hydrogel sensor was tested with different glucose solutions and the percentage increase in fluorescence intensity calculated and shows good response in the physiological range of glucose. The designed hydrogel sensor is ideal as a rapid bioanalyte assay for glucose.

6. FUTURE DIRECTIONS

The PEG SG-BSA hydrogel, immobilized with fluorophore and glucose oxidase enzyme is characterized by high water content, retention of immobilized enzyme activity and good fluorescence response and resolution in the physiological range of blood plasma glucose concentration.

The thermal analysis and mechanical analysis characterization data is indicative of the overall similar nature of the hydrogel matrix with and without the sensing elements (fluorophore and enzyme). The hydrogels are optically transparent, solids at room temperature and are of random copolymer type. There is no observed phase separation or loss in enzyme activity due to cross-linking to the hydrogel matrix. This hydrogel matrix (PEG SG-BSA) has tremendous potential to be tuned to sense a different analyte or molecule by incorporating appropriate sensing elements such as fluorophore or enzyme.

Besides the high water content, the use of 4-arm PEG SG in a FDA approved wound sealant, CoSeal® makes the designed hydrogel more likely to be biofouling and biocompatible to body tissues.

For human *in-vivo* use, the BSA component of the hydrogel should be replaced with HSA (Human serum albumin) to avoid potential immunogeneic reactions. Since the serum albumins have similar amine residues and stabilizing properties, the hydrogel properties could be similar at large.

Long-term *in-vivo* glucose monitoring for CGM applications requires the sensor to continuously sense plasma glucose concentration [59-60]. Previous studies of

fluorescent hydrogels that continuously sense glucose concentration both in *in-vivo* and *in-vitro* conditions are documented in literature. The designed hydrogel sensor should be tested for continuously varying glucose concentration in *in-vitro* and later *in-vivo* conditions.

Poly(ethylene glycol) is known to stabilize proteins and is extensively used in protein formulations and as drug delivery vehicles. With further *in-vivo* experiments to test the biocompatibility, swelling associated volume change in the hydrogel and drug loading and release experiments, the PEG SG-BSA hydrogels shows great promise for an *in-vivo* injectable, biodegradable hydrogel biosensing applications and have the potential in being used as drug delivery vehicle. Pipeline dream includes hydrogel sensing the plasma blood glucose concentration and release insulin to associated volume change.

7. REFERENCES

1. Association, A.D. *Diabetes Basics*. 2011 [cited 2014 May 5]; Available from: http://www.diabetes.org/diabetes-basics/statistics/.
2. Federation., I.D. *IDF diabetes atlas.* 2013 [cited 2014 May 5]; Available from: http://www.diabetesatlas.org/content/regional-data.
3. Group, T.D.C.a.C.T.R., *The Effect of Intensive Treatment of Diabetes on the Development and Progression of Long-Term Complications in Insulin-Dependent Diabetes Mellitus.* New England Journal of Medicine, 1993. **329**(14): p. 977-986.
4. Group, T.D.C.a.C.T.E.o.D.I.a.C.D.E.S.R., *Intensive Diabetes Treatment and Cardiovascular Disease in Patients with Type 1 Diabetes.* New England Journal of Medicine, 2005. **353**(25): p. 2643-2653.
5. Reach, G. and G.S. Wilson, *Can continuous glucose monitoring be used for the treatment of diabetes?* Analytical Chemistry, 1992. **64**(6): p. 381A-386A.
6. Newman, J.D. and A.P. Turner, *Home blood glucose biosensors: a commercial perspective.* (0956-5663 (Print)).
7. Klonoff, D.C., *Continuous Glucose Monitoring: Roadmap for 21st century diabetes therapy.* Diabetes Care, 2005. **28**(5): p. 1231-1239.
8. Deeb, L.C., *Diabetes Technology During the Past 30 Years: A Lot of Changes and Mostly for the Better.* Diabetes Spectrum, 2008. **21**(2): p. 78-83.
9. Wickramasinghe, Y., S.A. Yang Y Fau - Spencer, and S.A. Spencer, *Current problems and potential techniques in in vivo glucose monitoring.* (1053-0509 (Print)).
10. Oliver, N.S., et al., *Glucose sensors: a review of current and emerging technology.* Diabetic Medicine, 2009. **26**(3): p. 197-210.
11. Pickup, J.C., et al., *Fluorescence-based glucose sensors.* Biosensors and Bioelectronics, 2005. **20**(12): p. 2555-2565.
12. Steiner, M.-S., A. Duerkop, and O.S. Wolfbeis, *Optical methods for sensing glucose.* Chemical Society Reviews, 2011. **40**(9): p. 4805-4839.
13. James, T.D., *Boronic Acid-Based Receptors and Sensors for Saccharides*, in *Boronic Acids*. 2006, Wiley-VCH Verlag GmbH & Co. KGaA. p. 441-479.
14. Reeke, G.N., J.W. Becker, and G.M. Edelman, *The covalent and three-dimensional structure of concanavalin A. IV. Atomic coordinates, hydrogen bonding, and quaternary structure.* Journal of Biological Chemistry, 1975. **250**(4): p. 1525-1547.
15. Odaci, D., et al., *Fluorescence Sensing of Glucose Using Glucose Oxidase Modified by PVA-Pyrene Prepared via "Click" Chemistry.* Biomacromolecules, 2009. **10**(10): p. 2928-2934.
16. Clapp, A.R., et al., *Fluorescence Resonance Energy Transfer Between Quantum Dot Donors and Dye-Labeled Protein Acceptors.* Journal of the American Chemical Society, 2003. **126**(1): p. 301-310.
17. Chan, W.C.W., et al., *Luminescent quantum dots for multiplexed biological detection and imaging.* Current Opinion in Biotechnology, 2002. **13**(1): p. 40-46.
18. Vaddiraju, S., et al., *Technologies for continuous glucose monitoring: current problems and future promises.* Journal of Diabetes Science and Technology, 2010. **4**(6): p. 1540-1562.

19. Tanaka, T., *Collapse of gels and the critical endpoint.* Phys. Rev. Lett. , 1978. **40**(12): p. 820-823.
20. Tanaka, T.N., I.; Sun, S.-T.; Ueno-Nishio, *S. Collapse of gels in an electric-field. .* Science 1982. **218**: p. 467-469.
21. Irie, M.M., Y.; Tanaka, T. , *Stimuli-responsive polymers: chemical induced reversible phase separation of an aqueous solution of poly(N-isopropylacrylamide) with pendent crown ether groups. .* Polymer 1993. **34 (21)**: p. 4531 – 4535.
22. Gayet, J.C. and G. Fortier, *High water content BSA-PEG hydrogel for controlled release device: Evaluation of the drug release properties.* Journal of Controlled Release, 1996. **38**(2–3): p. 177-184.
23. Gayet, J.-C. and G. Fortier, *Drug Release from New Bioartificial Hydrogel.* Artificial Cells, Blood Substitutes and Biotechnology, 1995. **23**(5): p. 605-611.
24. Gerlach, G., *Hydrogel Sensors and Actuators : Engineering and Technology*. 2009, Springer: Dordrecht.
25. Peng, H.T., M.D. Blostein, and P.N. Shek, *Experimental optimization of an in situ forming hydrogel for hemorrhage control.* Journal of Biomedical Materials Research Part B: Applied Biomaterials, 2009. **89B**(1): p. 199-209.
26. Bhatia, S.K., *Biomaterials for Clinical Applications*. 2010, Springer: Dordrecht.
27. Wallace, D.G., et al., *A tissue sealant based on reactive multifunctional polyethylene glycol.* Journal of Biomedical Materials Research, 2001. **58**(5): p. 545-555.
28. Marc Hendrikx, M., et al., *Evaluation of a novel synthetic sealant for inhibition of cardiac adhesions and clinical experience in cardiac surgery procedures.* The heart surgery forum, 2001. **4**(3): p. 204-9; discussion 210.
29. Hongqi Li, L.C.a.Z.C., , DOI: 10.5772/33157., *Coumarin-Derived Fluorescent Chemosensors*. Advances in Chemical Sensors, ed. P.W. Wang. 2012: InTech.
30. Gismervik, B.C., *Fluorescence Tagging of Marine Low Molecular Weight Carboxylic Acids*. 2012.
31. SASAMOTO, K., et al., *Precolumn fluorescence derivatization of carboxylic acids using 4-aminomethyl-6, 7-dimethoxycoumarin in a two-phase medium.* Analytical sciences, 1996. **12**(2): p. 189-193.
32. Toyo'oka, T., *Fluorescent tagging of physiologically important carboxylic acids, including fatty acids, for their detection in liquid chromatography.* Analytica Chimica Acta, 2002. **465**(1): p. 111-130.
33. Robert-Peillard, F., et al., *Alternative spectrofluorimetric determination of Short-Chain Volatile Fatty Acids in aqueous samples.* Analytical Chemistry, 2009. **81**(8): p. 3063-3070.
34. Lim, N.C., et al., *Coumarin-based chemosensors for zinc (II): toward the determination of the design algorithm for CHEF-type and ratiometric probes.* Inorganic chemistry, 2005. **44**(6): p. 2018-2030.
35. Hirayama, K., et al., *Rapid confirmation and revision of the primary structure of bovine serum albumin by ESIMS and Frit-FAB LC/MS.* (0006-291X (Print)).
36. Mossavarali, S., et al., *Stepwise modification of lysine residues of glucose oxidase with citraconic anhydride.* International Journal of Biological Macromolecules, 2006. **39**(4–5): p. 192-196.

37. Raba, J. and H.A. Mottola, *Glucose Oxidase as an Analytical Reagent.* Critical Reviews in Analytical Chemistry, 1995. **25**(1): p. 1-42.
38. Lim, N.C., C. Pavlova Sv Fau - Bruckner, and C. Bruckner, *Squaramide hydroxamate-based chemidosimeter responding to iron(III) with a fluorescence intensity increase.* (1520-510X (Electronic)).
39. Li, L., et al., *In situ forming biodegradable electroactive hydrogels.* Polymer Chemistry, 2014. **5**(8): p. 2880-2890.
40. Dinu MV, O.M.M., Dragan E S, Okay O *Freezing as a path to build macroporous structures:super fast responsive polyacrylamide hydrogels.* Polymer (2007): p. 195–204.
41. *Chemical Engineering Methods and Technology : Fourier Transform Infrared Spectroscopy: Developments, Techniques and Applications*. 2010, New York, NY, USA: Nova Science Publishers, Inc.
42. Wang, C., et al., *DNA microarray fabricated on poly(acrylic acid) brushes-coated porous silicon by in situ rolling circle amplification.* Analyst, 2012. **137**(19): p. 4539-4545.
43. Chao, G., et al., *Preparation and Characterization of pH Sensitive Semi-interpenetrating Network Hydrogel Based on Methacrylic Acid, Bovine Serum Albumin (BSA), and PEG.* Journal of Polymer Research, 2006. **13**(5): p. 349-355.
44. Wunderlich, B., *THERMAL ANALYSIS TX Z*. 2012, Elsevier Science: Burlington.
45. Housmans, J.-W., G.M. Peters, and H.H. Meijer, *Flow-induced crystallization of propylene/ethylene random copolymers.* Journal of Thermal Analysis and Calorimetry, 2009. **98**(3): p. 693-705.
46. Gayet, J.-C., P. He, and G. Fortier, *Bioartificial Polymeric Material: Poly(Ethylene Glycol) Crosslinked with Albumin. II: Mechanical and Thermal Properties.* Journal of Bioactive and Compatible Polymers, 1998. **13**(3): p. 179-197.
47. Bair, H.E., et al., *Thermomechanical Analysis (TMA) and Thermodilatometry (TD)*, in *Thermal Analysis of Polymers*. 2008, John Wiley & Sons, Inc. p. 319-385.
48. Wang, P., et al., *Preparation and characterization of a novel hybrid copolymer hydrogel with poly(ethylene glycol) dimethacrylate, 2-hydroxyethyl methacrylate and layered double hydroxides.* Journal of Shanghai Jiaotong University (Science), 2012. **17**(6): p. 712-716.
49. Kiskan, B. and Y. Yagci, *Thermally curable benzoxazine monomer with a photodimerizable coumarin group.* Journal of Polymer Science Part A: Polymer Chemistry, 2007. **45**(9): p. 1670-1676.
50. Peppas, N.A., Hydrogels in Medicine and Pharmacy, Vol. I: Fundamentals. 1986, and C.P.B. Raton.
51. Zhang, X.-Z., P. Jo Lewis, and C.-C. Chu, *Fabrication and characterization of a smart drug delivery system: microsphere in hydrogel.* Biomaterials, 2005. **26**(16): p. 3299-3309.
52. Bryant, S.J., J.A. Arthur, and K.S. Anseth, *Incorporation of tissue-specific molecules alters chondrocyte metabolism and gene expression in photocrosslinked hydrogels.* Acta Biomaterialia, 2005. **1**(2): p. 243-252.
53. Drury, J.L., R.G. Dennis, and D.J. Mooney *The tensile properties of alginate hydrogels.* Biomaterials, 2004. **25(16)**: p. 3187-3199.

54. Chivukula, P., et al., *Synthesis and characterization of novel aromatic azo bondcontaining pH-sensitive and hydrolytically cleavable IPN hydrogels.* Biomaterials 2006. **27**(7): p. 1140-1151.
55. Brondsted, H.a.J.K., *Hydrogels for site-specific oral drug delivery: synthesis and characterization.* Biomaterials 1991. **12**(6): p. 584-592.
56. Coviello, T., et al., "A new polysaccharidic gel matrix for drug delivery:, preparation and mechanical properties". Journal of Controlled Release, and p. 643-656.
57. Gulrez, S.K.H. and S. Al-Assaf, *Hydrogels: Methods of Preparation, Characterisation and Applications*. Progress in Molecular and Environmental Bioengineering - From Analysis and Modeling to Technology Applications. 2011.
58. Chartoff, R.P., J.D. Menczel, and S.H. Dillman, *Dynamic Mechanical Analysis (DMA)*, in *Thermal Analysis of Polymers*. 2008, John Wiley & Sons, Inc. p. 387-495.
59. Vilozny, B., et al., *Multiwell plates loaded with fluorescent hydrogel sensors for measuring pH and glucose concentration.* Journal of Materials Chemistry, 2011. **21**(21): p. 7589-7595.
60. Suri, J.T., et al., *Continuous Glucose Sensing with a Fluorescent Thin-Film Hydrogel.* Angewandte Chemie International Edition, 2003. **42**(47): p. 5857-5859.